

# Omnidirectional camera

Mika Aikio, Jukka-Tapani Mäkinen  
Optical Instruments  
VTT Technical Research Center of Finland  
Oulu, Finland  
Mika.Aikio@vtt.fi

Bo Yang  
University of Shanghai for Science and Technology  
Shanghai, China

**Abstract**— We investigated the possibility of adding a wide-angle converter lens on top of an existing mobile phone camera to provide a 360 degree image of the surroundings of the phone. The motivation behind this work is a possibility of a video stream from a meeting where every participant would be imaged at the same time with sufficient resolution, eliminating the need for separate conferencing equipment. While it is true that the same could be achieved with a fish-eye lens, we believe that our solution is unique and has certain advantages over the fish-eye lens in manufacturing and also in specific imagery cases.

**Keywords**— *Omnidirectional imaging, panoramic lens, mobile phone add-on device, mass production*

## I. INTRODUCTION

Omnidirectional imaging is a well-established imaging optics area, where multiple approaches are used to solve problems related to the large field size, attaining sufficient resolving power while keeping the distortion well under control to name a few. Additionally, ease of manufacturing is also an important consideration, which usually means to reduce the number of components.

Typically, objectives having larger fields of views are divided on to two separate branches, objectives yielding a rectilinear image and curvilinear image. Rectilinear image is typically the case for photographic wide-angle objectives. Currently for a 35 mm sensor, shortest marketed focal length is about 12 millimeters, resulting in a diagonal field of view of about 122 degrees. For smaller sensor sizes, 141 degree field of view objectives are available, but not much more than that are available on the consumer markets.

One important point is to note that for the 35 mm sensor, 12 mm focal length has the aperture ratio of 4.5, which is a relatively slow lens. Additionally, the object surface of the rectilinear is a flat plane if the field curvature is kept at low levels. So, for a rectilinear lens in the absence of distortion, the relation between the field angle and the image height is given by

$$h = f * \tan(\theta) \quad (1)$$

Here  $h$  is the image size,  $f$  is the focal length and  $\theta$  is the field angle. Given the tangential relationship between the image size and the field angle, it is seen that image size approaches infinity if  $\theta$  approaches 90 degrees. In other

words, it is not physically possible to provide rectilinear image for field angles greater than 180 degrees, and there must be distortion included. While there is several different distortion mapping methods, the most common is the equi-distance angle mapping, described by (2).

$$h = f * \theta \quad (2)$$

Here  $h$  is the image height,  $f$  is the focal length and  $\theta$  is the corresponding field of view. Now, it is apparent that with this mapping, there is a linear correspondence between the field angle and the image height.

The most typical objective providing curvilinear image is a fish-eye lens, though there are more optical constructs here as same applications require greater fields of views than possible with rectilinear objectives. Another typical approach, specifically in autonomous devices, is to have a standard machine vision objective and a convex mirror in front of it to expand the field of view [1, 2, 3, 4]. This approach yields a rather large field of view, but results typically large mirror sizes.

In optical design, an optical system consisting of refractive and reflective surfaces is called catadioptric, and the above mentioned camera lens and a mirror combination is one example of it. The distortion in these optical constructs is measured against the mapping provided by (2), and differs considerably from the distortion measured against (1).

Recently, some authors have investigated the possibility of using rotationally symmetric catadioptric lenses where the mirror in the front element is split to two or more surfaces to reduce the size of the system [5, 6]. At this point, it is important to consider also the typical object surface in the curvilinear objectives. A fish-eye lens has a spherical object surface, and the fact that fish-eye lenses distort straight lines can be attributed to this fact. For mirror and objective lens combinations, the object surface is curved, but the exact shape of the surface may be closer to a hyperboloid or a paraboloid. The difference from the cylindrical object surface is usually negligible, but may become important when using faster aperture ratios with corresponding drop in the depth of field.

It should be mentioned that in catadioptric constructs, the middle part of the image contains the shadow of the objective itself, and therefore cannot be used. In catadioptric systems employing multiple reflective surfaces, it is possible to have a

This work was done in MUSUVA-project, supported by TEKES, the Finnish Funding Agency for Technology and Innovation

cylindrical object surface, which is beneficial in the mobile conferencing application. It is our judgment that this configuration is closest to our imaging case from the listed wide-angle constructs.

Additionally, the application does not require visualizing large vertical fields of views; when the mobile phone add-on device is placed on the conference table, the upper body of the average participant is visible in about 30 degrees vertical field of view at the distance of 1.5 meters if the participant is sitting. The problem is the camera module in a mobile phone is designed to see directly upwards, and not sideways as would be needed in this application, and for that we propose a catadioptric add-on piece to be placed on the mobile phone camera.

## II. DESIGN OF THE OMNIDIRECTIONAL LENS SYSTEM

There is a myriad of different cameras in the mobile phones, and it is equally difficult to find public information on the construct of them, or their optical performance. These quantities cannot be measured from the photos of the mobile phone, as it is very likely that software correction is used for some optical aberrations. For this reason, authors decided to use a paraxial thin lens model for the mobile phone camera, and design the rest of the system in accordance with it to provide best possible commonality.

Our approach was to select a focal length of 5 millimeters and an F-number of 2.8, which by (1) would result in an image size of 6 millimeters with 60 degrees field of view, which we estimate, is close enough to the actuality. The aperture stop of the mobile phone camera lenses is usually ahead of all lens elements, yielding a short camera, a desirable property for mobile phones. Assuming that the sensor has a 4:3 form factor, it is relatively simple to calculate the shorter side length of the sensor, yielding 3.6 millimeters. Due to resulting circular symmetry, the entire image has to stay within this 3.6 millimeter diameter. If the sensor size is too small, some information on the lower angles (closest to horizontal plane) would be lost. If the image is too small with respect to this sensor size, then some information will be lost since not all pixels will be used by the image.

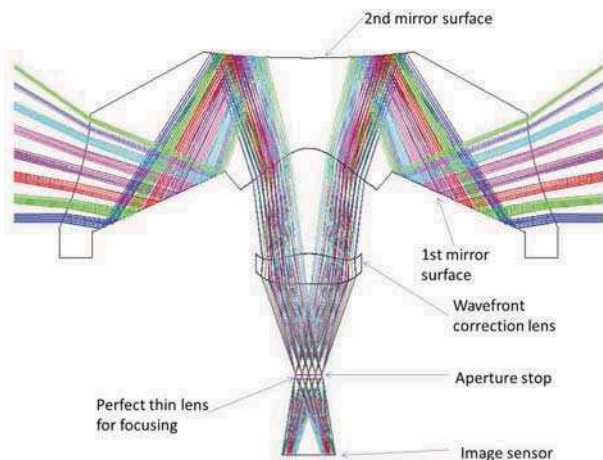


Fig. 1. Designed omnidirectional sensor with a thin lens objective.

The design path leading to the realized system (Fig. 1) is relatively complicated, but for a short review, a single mirror added on top of the phone camera lens does not work very well due to size and support mechanics, additionally the mirror shape tolerances may become prohibitive in mass production. One design step has been formerly published in [7].

For image quality reasons, the single mirror surface was split onto two reflective surfaces and instead of using air in the intermediate material, we selected optical plastic Zeonex E48R, which would enable us to do a single piece construction with the later possibility of injection molding. The side effect of this decision is that two additional refractive surfaces are needed to enclose the volume, and these surfaces can then be used in aberration control.

It was also discovered that due to the nature of the application, an additional corrective lens had to be placed in the optical path to control the imaging quality, without this lens, it was not possible to achieve sufficient drawing capability on the design phase. Our more recent work in this field hints that this lens may not be necessary on all cases.

The design performance of the realized optical system is listed on Table 1.

TABLE I. DESIGN PARAMETERS OF OMNIDIRECTIONAL SYSTEM

Light collection power	F/3.1
Focal length <sup>a</sup>	1 mm
Vertical field of view <sup>b</sup>	35 °
Resolution	100 lp/mm
Add-on piece diameter	35 mm
Add-on piece height	25 mm

<sup>a</sup> Focal length is given by the best fit of distortion to the mapping function (2).

<sup>b</sup> Vertical field of view is measured from the horizontal plane in this case. 35 degrees is measured from the horizontal plane. The vertical field of view is thus limited between 55 degrees and 90 degrees from the vertical axis.

The design was then sent for single point diamond turning, manufacturer being Kaleido Technologies from Denmark. Total of two add-on pieces with complete optics were manufactured.

## III. NOTES ON THE DESIGN

Little information is published on how to actually design these types of catadioptric omnidirectional lenses, despite a couple of related patents [6, 8-14], authors are only aware of work done by Gimkiewicz et al [5] where the lens was fabricated and measured. Of the patents, only in [11] the optical performance curves are disclosed. For single mirror surfaces, the theoretical and practical understanding is better documented [1-4]. As to this date, authors are not aware that there would be ready off-the-shelf components of these lenses available on the markets.

From the design point of view, it is clear by looking at Figure 1, that this type of an add-on piece will always have a

reflective conical surface somewhere in it. This surface cross-couples the tangential and sagittal optical power, and leads to several design complications. Unlike, for example, with a fast and slow axis cylindrical lenses used in fiber coupling, this case a single change in either the diameter of the cone or the apex angle of the cone will cause changes in both the tangential and sagittal performance of the system. This leads to the conclusion that the configuration is prone to astigmatism (differing spot sizes regarding tangential and sagittal axes) and coma (comet like appearance of the spot), and the job of the optical design is to minimize these effects as well as possible.

Additionally, some care should be placed on the control of the lateral color, while there are two reflective surfaces on the optics that do the majority of the work, there are still two refractive surfaces that contribute on the lateral color characteristics. By looking in Table 1, it is also seen that the aperture ratio has slightly decreased from the original F/2.8 of the camera phone. This is attributed to two factors, first is that the conical surface functions as a convex mirror, and spreads light. The light must then be collected by the rest of the optics, and still provide sufficient correction over the field of view.

Additionally, a length restriction was placed so that the supporting structure of the add-on piece would not protrude far from the mobile phone, and this is accomplished by having the beam of light slightly diverge when it enters the lens. This is equivalent of having a closer focus, and this changes the working aperture ratio slightly.

In our work related to omnidirectional lenses, we have not been able to keep the original aperture ratio throughout the system and because of the reasons listed above; we are yet to find a way to keep the original aperture ratio and still provide sufficient image quality. It is our experience from the design that the objective lens after the omnidirectional lens should have its aperture stop as close as possible to the add-on package. This eases the design work considerably, but also tends to limit this optical construct for smaller sensor sizes; common larger sensor objectives (e.g. C-mount) typically use structures derived from Double Gauss design, which makes the design more difficult because of the preceding lens elements can affect the beam more before the aperture stop.

#### IV. PERFORMANCE ANALYSIS

This section is devoted to the analysis of the simulated performance curves. The reason for this is simply that there are too many unknowns to reliably attribute each change in the measured performance to a single factor. These unknown factors are, for example, the mobile phone camera and the sensor themselves. Some experimental difficulty arose from the fact that the mobile phone mount itself was not correctly aligned with the optical axis of the camera and we could not correct this mechanically. As a result, there is a slight blurriness in one corner.

Some manufacturing technique related complications arose as well; diamond turning produces a periodic structure on the optical surface, which leads to slight diffraction effects that make characterizing some of the performance parameters difficult, specifically Modulation Transfer Function (MTF) is affected.

Figure 2 is the optical path difference (OPD) graph with respect to the normalized pupil coordinates for three different field angles. The graph with respect to pupil x-coordinate is symmetric, but shows different wavelengths (Fraunhofer F, d and C lines) at different places and the curve is typically of fourth order by nature. This means that there is some residual chromatic aberration left, and that in this direction, the major contributing aberration is spherical aberration. There is between -0.5 to 1.5 waves of it remaining, curiously the maximum of wavefront error in the pupil x-direction is achieved at the intermediate field angle, 17.5 degrees from the horizontal plane. The left side of the graph shows the wavefront error with respect to pupil y-coordinate, and this graph is non-symmetric. Third order functional behavior hints at coma being the worst offender along this axis, along with color aberrations. Reader is asked to note the scale of the graphs; the wavefront error is seen to start from -1.5 waves to 2.5 waves, about two times more than in the x-direction.

The fact that the graphs also differ in x- and y-axes tells that astigmatism is present. Despite all this, the correction is sufficient to achieve 100 lp/mm resolving power after tolerances. We would like to point out that the minimum in y-direction aberration is actually achieved in the same intermediate field angle as the x-direction achieves its maximum and they are about the same, which hints that the spot will be close to circular within this field angle and this is indeed the case.

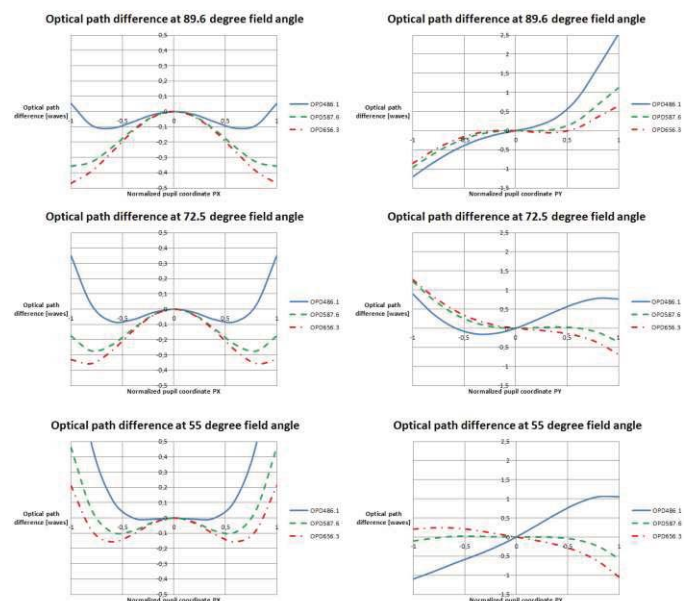


Fig. 2. Optical Path Difference graphs along pupil x- and pupil y-directions

The graph of lateral color is presented in Fig. 3. The behavior of lateral color is even in the respect that it never changes its sign. The designed maximum error of about 5.7  $\mu\text{m}$  equals about 2 pixels in this class of camera phones, and during the usage in general photography, we did not find the lateral color itself being present in the photographs. However, much bigger deviation in color graphs is attributed to the diamond turning grooves, which do produce rainbow patterns on the

proximity of areas with high contrast differences. In our measurements, we found the period of the grooves to be around 6  $\mu\text{m}$ , and their amplitude was about 20 nm, surface roughness (Rq) value was measured to be around 30 nm RMS with a white light interferometer. Little information on modeling the diamond turned grooves in optics is publicly available [15], and the estimation of their effect on the total performance is comparatively difficult.

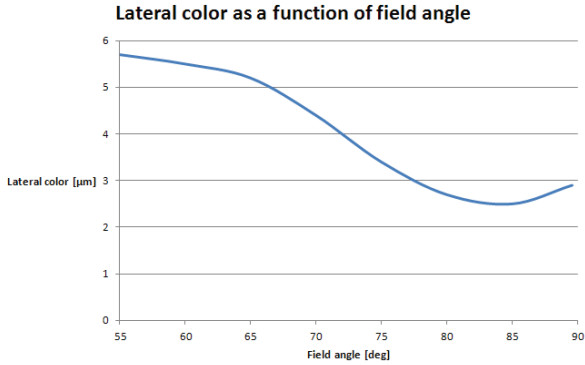


Fig. 3. Lateral color as a function of field angle

The field angle versus the position on sensor graph and the calibrated distortion graph are represented in Figs. 4 and 5.

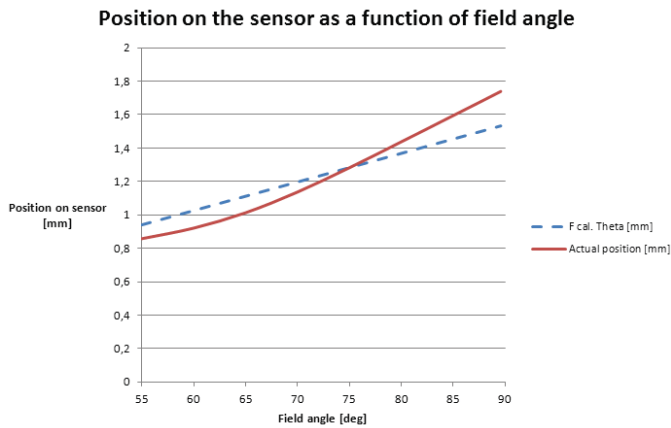


Fig. 4. Position on the sensor as a function of field angle for 1 mm fish-eye lens given by (2) and the actual realized system.

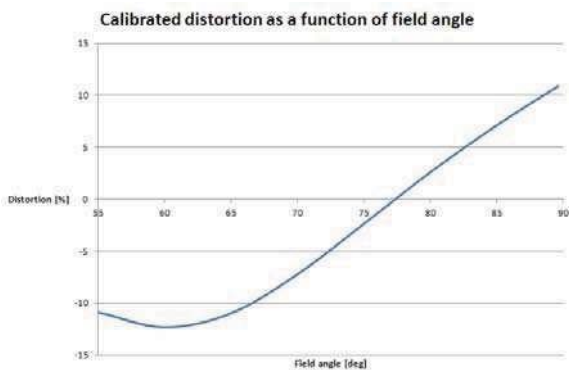


Fig. 5. Calibrated distortion with respect to 1 mm focal length equi-distance projection lens as a function of field angle.

The distortion graph has been calculated using (3),

$$D(\theta) = \frac{H_y(\theta) - H_m(\theta)}{H_y(\theta)} * 100 \% \quad (3)$$

Here  $H_y$  is the nominal position for a field angle given by (2), and  $H_m$  is the actual measured position. The best fit focal length can be obtained from by minimizing the error between measured data and the positions given by (2). Thus our optical omnidirectional camera system has an equivalent focal length of one millimeter to the equi-distance mapping fish-eye lens. It can be seen from the Fig. 2 that there is a departure from the nominal position, resulting the calibrated distortion being between -15 % and + 10 % values depending on the field angle. The authors believe that this kind of lens allows different kind of control on the distortion characteristics, which may be of advantage on some cases.

## V. DISCUSSION

A proof-of-concept omnidirectional lens was designed and manufactured, and the overall design was found to be functional and feasible with regards to manufacturing. Several manufacturing issues were discovered, including uncertainty with regards to the mobile phone camera, but the most serious of them were related to the diamond turning process itself, and are expected to be remedied in the injection molding process which uses super polished master elements.

For future work, we are already preparing a new run of the optics which doubles the vertical field of view, and uses 7 mm diagonal sensor with custom made objective lens. In this case, we are able to eliminate the uncertainty regarding the exact type of the objective lens and optical alignment, but no measurement results are available, but we look forward on reporting them in the future as they become available.

## ACKNOWLEDGMENT

Authors would like to thank Kaleido Technologies for providing the omnidirectional lenses and for the good discussion of the manufacturability of the components. Additional thanks go to Dr. Mauri Aikio, who initially drafted the MUSUVA project, and to Professor Qinsheng He for the arrangements during the researcher exchange periods.

This paper is written within PAN-Robots project. PAN-Robots is funded by the European Commission, under the 7th Framework Programme Grant Agreement n. 314193. The partners of the consortium thank the European Commission for supporting the work of this project.

## REFERENCES

- [1] K. Yamazawa, Y. Yagi, and M. Yachida, "Omnidirectional imaging with hyperboloidal projection," Proceedings of the 1993 IEEE/RSJ International Conference on Intelligent Robots and Systems, pp. 1029-1034.
- [2] S. Hrabar and G. Sukhatme, "Omnidirectional Vision for an Autonomous Helicopter," Proceedings of the IEEE International

- Conference on Robotics and Automation (ICRA03), 2004, pp. 3602-3609.
- [3] H. Ishiguro, "Development of low-cost compact omnidirectional vision sensors and their applications," Proceedings of the International Conference on Information Systems, Analysis and Synthesis, 1998, pp. 433-439.
- [4] A. Ohte and O. Tsuzuki, "Practical design and evaluation methods of omnidirectional vision sensors," *Optical Engineering*, Vol. 51(1), 2012.
- [5] C. Gimkiewicz et al., "Ultra-miniature catadioptrical system for an omnidirectional camera," Proc. SPIE 6992, Micro-Optics 2008, 69920J (May 03, 2008).
- [6] E. Gal, G. Liteyga and G. Graisman, "Omni-directional imaging and illumination assembly," US Patent 7,570,437 B2, August 4, 2009.
- [7] B. Yang, et al., "Free-form lens design for wide-angle imaging with an equidistance projection scheme", *Opt. Int. J. Light Electron. Opt.* 2007.
- [8] E. Gal, "Spherical and nearly spherical view imaging assembly," US Patent 7,253,969 B2, August 7, 2007.
- [9] E. Gal, G. Graisman, G. Liteyga, "Optical lens providing omnidirectional coverage and illumination", US Patent 7,362,516 B2, April 22, 2008.
- [10] M. J. Mandella, "Solid catadioptric lens with a single viewpoint", US Patent 2005/0111084 A1, May 26, 2005.
- [11] T. Togino, "Optical System", US Patent 2008/0151380 A1, June 26, 2008.
- [12] T. Doi, "Panoramic imaging lens", US Patent 2003/0099045 A1, May 29, 2003.
- [13] I. Powell, "Panoramic lens", US Patent 5,473,474, December 5, 1995.
- [14] T. Togino, "Optical System", Japanese Patent JP2006243689A, June 26, 2008.
- [15] H. Chunning, "Investigation of injection molding process for high precision polymer lens manufacturing", Ph. D. dissertation in Industrial and Systems Engineering Graduate Program, Ohio State University, 2008.